Int J Fract (2006) 141:535–547
DOI 10.1007/s10704-006-9012-y

ORIGINAL PAPER

An analytical approach for fracture and fatigue in functionally graded materials

Alberto Carpinteri · Marco Paggi · Nicola Pugno

Received: 16 January 2006 / Accepted: 27 July 2006 / Published online: 25 October 2006
© Springer Science+Business Media B.V. 2006

Abstract The problem of brittle crack propagation and fatigue crack growth in functionally graded materials (FGMs) is addressed. The proposed analytical approach can be used to estimate the variation of the stress-intensity factor as a function of the crack length in FGMs. Furthermore, according to the Paris' law, the fatigue life and the crack-tip velocity of crack propagation can be predicted in the case of fatigue crack growth. A comparison with numerical results obtained according to the Finite Element method will show the effectiveness of the proposed approach. Detailed examples are provided in the case of three-point bending beam problems with either a FGM interlayer, or a FGM external coating. A comparison is presented between two types of grading in the elastic modulus: a continuous linear variation in the FGM layer and a discrete approximation with a multi-layered beam and a constant Young's modulus in each layer.

A. Carpinteri(✉) · M. Paggi · N. Pugno
Department of Structural and Geotechnical Engineering,
Politecnico di Torino,
Corso Duca degli Abruzzi 24,
Torino 10129, Italy
e-mail: alberto.carpinteri@polito.it

M. Paggi
e-mail: macro.paggi@polito.it

N. Pugno
e-mail: nicola.pugno@polito.it

Keywords Functionally graded materials · Multi-layered elements · Brittle crack propagation · Fatigue crack growth

1 Introduction

Functionally graded materials (FGMs) have been designed to overcome the drawbacks due to an abrupt variation of the mechanical properties occurring at interfaces and material junctions (see e.g., Erdogan 1995; Erdogan and Wu 1997; Jin and Batra 1996; Carpinteri and Paggi 2005, among others). They consist in one material on one side and a second material on the other, connected by an intermediate layer with a continuous inhomogeneity of composition or structure. FGMs arose from a unique idea for realization of innovative properties that cannot be achieved by conventional isotropic materials.

A collection of technical papers that represents current research interests with regard to the fracture behavior of FGMs has been recently proposed (Paulino 2002). It has been shown that for crack problems in FGMs the crack-tip has a regular square-root singularity and stress and displacement fields have the same form as those of the homogeneous materials (Eischen 1987). In these problems, the influence of the material gradients manifests itself through the stress-intensity factors. The Finite Element method is usually applied to

solve these problems and it is the most useful and often-used approach to model fracture in FGMs (Gu et al. 1999; Kim and Paulino 2002, 2003). Very often, due to the complexity of the problem, closed-form solutions provided by theoretical models involve complex mathematical procedures (Delale and Erdogan 1983; Fett and Munz 1997). Recently, Carpinteri and Pugno (2005, 2006) have proposed an approximate analytical approach which permits to handle with nonhomogeneous three-point bending beams and plates in extension, confirmed by Finite Element simulations in case of multi-layered elements (Carpinteri et al. 2006).

Starting from Carpinteri and Pugno (2005, 2006), the mathematical formulation is herein briefly revised and particularized to the geometry of three-point bending specimens having either a FGM interlayer, or a FGM external coating. To show the effectiveness of the proposed approach, a comparison with Finite Element results is proposed. In addition to previous published results, the problem of fatigue crack growth in FGMs is addressed. Two types of grading are considered: the former corresponds to a linear variation of the elastic modulus along the FGM layer depth, whereas the latter consists in a discrete approximation with a constant elastic modulus equal to the average value of the Young's moduli of the connected layers. In the sequel, these configurations will be referred to as continuous and discrete grading, respectively. A detailed comparison between these two possible technical solutions is presented.

2 Fracture in FGMs

Let us consider a three-point bending beam composed of a heterogeneous material whose elastic modulus varies along its depth (see the scheme in Fig. 1a).

For the corresponding homogeneous structure, i.e., $E(y) = \text{const}$, the Mode I stress-intensity factor, K_{I}, is given by:

$$K_{\mathrm{I}} = \frac{4M}{bh^{3/2}} f\,(a/h)\,, \tag{1}$$

where M is the bending moment in the cracked section, b is the width (along the x-axis), h is the total depth of the beam (along the y-axis) and a is the

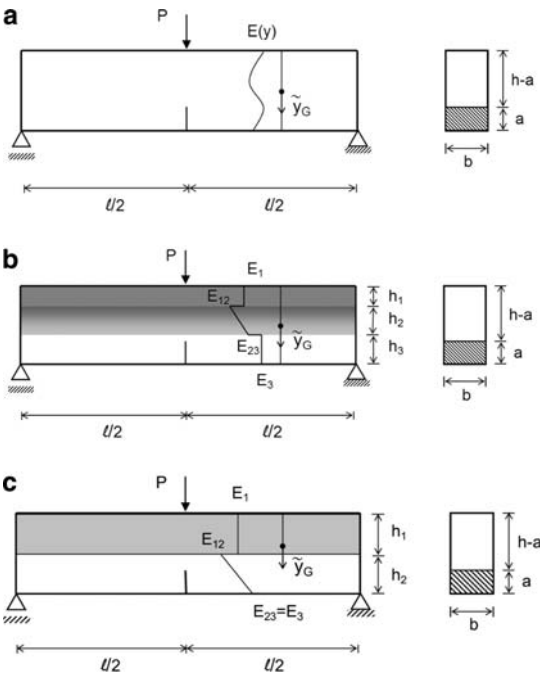

Fig. 1 Schemes of three-point bending beams (**a**) with a given grading in the elastic modulus; (**b**) composed of three-layers with a FGM interlayer; (**c**) composed of two layers with an external FGM layer

crack depth. The shape function f can be expressed as follows ($a/h < 0.6$) (Murakami 1987):

$$f\left(\frac{a}{h}\right) = 2.9\left(\frac{a}{h}\right)^{1/2} - 4.6\left(\frac{a}{h}\right)^{3/2} + 21.8\left(\frac{a}{h}\right)^{5/2} - 37.6\left(\frac{a}{h}\right)^{7/2} + 38.7\left(\frac{a}{h}\right)^{9/2}. \tag{2}$$

Brittle crack propagation arises when the bending moment is such that $K_{\mathrm{I}} = K_{\mathrm{IC}}$, at the crack-tip:

$$M_{\mathrm{C}} = \frac{K_{\mathrm{IC}} bh^{3/2}}{4f\,(a/h)}, \tag{3}$$

For functionally graded materials we look for a solution of the stress-intensity factor in a form similar to Eq. 1:

$$\widetilde{K}_{\mathrm{I}} = \frac{4\widetilde{M}}{bh^{3/2}} \widetilde{f}\,(a, h, E(y))\,, \tag{4}$$

where $(\sim)$ denotes a quantity in the structure with FGM and the shape function $\widetilde{f}$ is the main unknown that we are looking for. Also in this case, brittle crack propagation will arise when $\widetilde{M} = \widetilde{M}_{\mathrm{C}}$, corresponding to the condition of $\widetilde{K}_{\mathrm{I}} = \widetilde{K}_{\mathrm{IC}}$ at the crack-tip. In this formulation, $\widetilde{K}_{\mathrm{IC}}$ denotes the critical value for the stress-intensity factor of the FGM

evaluated at the crack-tip. Function $\widetilde{f}$ must satisfy the following limit case for the self-consistency of the theory:

$$\widetilde{f}\,(a,h,E(y)=\text{const})=f\left(a/h\right) \tag{5}$$

For a given Young's modulus profile, $E(y)$, this function can be obtained numerically, as usually done for f in the homogeneous case (Gu et al. 1999).

The mechanical behavior of structures with cracks or re-entrant corners can be described by the brittleness number, $\widetilde{s}=\widetilde{K}_{\mathrm{IC}}/\left(\widetilde{\sigma}_u b^{(1-\lambda)}\right)$, introduced by Carpinteri (1982, 1987) for homogeneous structures and then extended by Carpinteri et al. (2006) to multi-layered elements. The exponent λ defines the power of the stress-singularity at the crack-tip and it is equal to $1/2$ for a crack inside homogeneous and FGM structures, whereas it depends on the elastic mismatch for a crack meeting a bi-material interface in layered structural components. In general, larger the brittleness number $\widetilde{s}$, larger the structural ductility. If this number is beyond a characteristic threshold, the ductile collapse ($\widetilde{\sigma}=\widetilde{\sigma}_{\mathrm{u}}$) precedes the generalized brittle collapse ($\widetilde{K_{\mathrm{I}}}=\widetilde{K_{\mathrm{IC}}}$) for any relative crack depth. Then, considering a nonlocal fracture stress criterion to overcome the paradox between the tensional and the energy approaches, a relationship between the brittleness number for a heterogeneous structure and that for a homogeneous element can be established (Carpinteri and Pugno 2005, 2006). This relationship can be further manipulated by considering the relationships between the brittleness numbers and the applied bending moments either for crack propagation or for tensional collapse for homogeneous and heterogeneous structural elements, leading to the following similarity equation:

$$\frac{\widetilde{M}_{\mathrm{C}}}{M_{\mathrm{C}}}\approx\frac{\widetilde{M}^{\mathrm{t}}_{\mathrm{C}}}{M^{\mathrm{t}}_{\mathrm{C}}} \tag{6}$$

where $M^{\mathrm{t}}_{\mathrm{C}}$ and $\widetilde{M}^{\mathrm{t}}_{\mathrm{C}}$ denote, respectively, the bending moment of first plastic deformation for a homogeneous beam, which is the maximum moment in the elastic regime when tensional collapse ($\sigma_{\max}=\sigma_{\mathrm{u}}$) takes place:

$$M^{\mathrm{t}}_{\mathrm{C}}=\frac{\sigma_{\mathrm{u}}bh^2}{4g\,\left(a/h\right)}, \tag{7}$$

and the bending moment of first plastic deformation for the heterogeneous beam:

$$\widetilde{M}^{\mathrm{t}}_{\mathrm{C}}=\frac{\widetilde{\sigma}_{\mathrm{u}}bh^2}{4\widetilde{g}\,(a,h,E(y))}. \tag{8}$$

Parameter σ_{u} is the ultimate strength of the material in the homogeneous structure, whereas $\widetilde{\sigma}_{\mathrm{u}}$ is the ultimate strength of the material evaluated at the crack-tip for the heterogeneous case. Functions g and $\widetilde{g}$ are known functions and can be easily computed.

A numerical assessment of this proportionality relationship is proposed for the bi-layered beam sketched in Fig. 1c with different values of the modular ratios, E_2/E_1 ($E_3=E_{23}=E_{12}E_2$), with $h_2/h_1=2/3$, and with different crack depths, a/h, using the Finite Element procedure as described in Carpinteri et al. (2006). According to this approach, the ratio R between the first and second member of Eq. 6 is numerically computed and the results are reported in Table 1. As it can be seen,

Table 1 Numerically computed values of the ratio R for the bi-layered beam in Fig. 1c with $h_2/h_1=2/3$ using the finite element method

R	a/h	0.05	0.10	0.15	0.20	0.25	0.30	0.35	0.40	0.45	0.50	0.55	0.60	0.65	0.70
E_2/E_1															
0.10		0.97	1.05	1.13	1.21	1.28	1.35	1.36	0.42	0.83	0.92	0.96	0.98	1.00	1.03
0.20		0.97	1.02	1.07	1.12	1.18	1.24	1.27	0.52	0.88	0.94	0.97	0.98	1.00	1.03
0.40		0.97	0.99	1.02	1.05	1.08	1.12	1.15	0.68	0.93	0.96	0.98	0.99	1.00	1.03
0.80		0.98	0.99	0.99	1.00	1.01	1.02	1.03	0.91	0.98	0.99	0.99	0.99	1.00	1.03
1.00		1.00	1.00	1.00	1.00	1.00	1.00	1.00	1.00	1.00	1.00	1.00	1.00	1.00	1.03
1.25		0.99	1.00	1.00	1.00	0.99	1.05	1.05	0.87	1.08	1.08	0.99	0.99	1.00	1.03
2.50		1.02	1.03	1.03	1.03	1.00	0.96	0.88	1.32	1.04	1.01	1.00	0.99	1.01	1.03
5.00		1.04	1.06	1.08	1.10	1.09	1.03	0.87	1.48	1.07	1.02	1.00	1.00	1.01	1.03
10.00		1.03	1.07	1.12	1.18	1.21	1.17	0.94	1.46	1.09	1.03	1.01	1.00	1.00	1.03

the computed ratio is close to the unity, as predicted by the approximate relationship.

Equation 6 permits to derive a simple closed-form estimation of $\widetilde{f}$. To be more specific, starting from the evaluation of $\widetilde{g}\,(a,h,E(y))$, we assume the conservation of plane (ligament) cross-sections after deformation, as usually considered in the study of multi-layered beams in bending (see e.g., Carpinteri 1997; Chawla 1987). The assumption of conservation of plane sections holds, provided that the different materials are securely bonded together so as to give the necessary resistance to longitudinal shearing stresses. This hypothesis implies a linear (along the y co-ordinate) axial (z) dilation. The stress results to be nonlinear (along y) and can be evaluated as follows (Carpinteri 1997):

$$\sigma_z\,(y) = \frac{E(y)M}{\widetilde{E}I_x^*}y, \tag{9}$$

where $\widetilde{E}$ is the Young's modulus of the material at the crack-tip, and:

$$I_x^* = \int\limits_{A_{\rm lig}} \frac{E(y)}{\widetilde{E}}y^2 {\rm d}A \tag{10}$$

is the weighted moment of inertia. The integral in Eq. 10 is performed over the ligament cross-sectional area, $A_{\rm lig}$. The origin of the chosen reference system for the subsequent analysis is placed at the centroid of the composite cross-section, defined by the condition of a vanishing weighted static moment (see Carpinteri 1997):

$$S_x^* = \int\limits_{A_{\rm lig}} \frac{E(y)}{\widetilde{E}}y {\rm d}A = 0, \tag{11}$$

In this computation, the use of an equivalent or transformed cross-section for a beam of homogeneous material is made. The transformed section is simply obtained by replacing either material by an equivalent amount of the other material as determined by the ratio of their elastic moduli. Once this centroid is determined, then this is chosen as the origin of the reference system and the position of the crack-tip, $\widetilde{y}$, is computed with respect to that datum (examples of application are reported in the Appendix).

From the previous equations it follows:

$$\widetilde{g}\,(a,h,E(y)) = \frac{bh^2\widetilde{y}}{4\widetilde{I}_x^*}. \tag{12}$$

For a homogeneous structure we have $\widetilde{y}=(h-a)/2$ and Eq. 12 reduces to:

$$g\left(a/h\right) = \widetilde{g}\,(a,h,E(y)={\rm const}) = \frac{3/2}{(1-a/h)^2}. \tag{13}$$

Introducing Eqs. 2, 12 and 13 into Eq. 6, we obtain an estimation of the unknown shape function for FGMs (Carpinteri and Pugno 2005, 2006):

$$\widetilde{f}\,(a,h,E(y)) = \frac{\sigma_{\rm u}\widetilde{K}_{\rm IC}}{\widetilde{\sigma}_{\rm u}K_{\rm IC}}\frac{\widetilde{g}\,(a,h,E(y))}{g\left(a/h\right)}f\left(a/h\right). \tag{14}$$

Summarizing, for a given material grading, we have to evaluate $\widetilde{y}$ and I_x^* in order to compute $\widetilde{g}$ and g. Then, the generalized shape function $\widetilde{f}$ is worked out. Consequently, a prediction of the generalized stress-intensity factor $\widetilde{K}_{\rm I}$ for the FGM problem can be obtained. A further simplification will be introduced in the sequel by considering $\sigma_{\rm u}\widetilde{K}_{\rm IC} \cong \widetilde{\sigma}_{\rm u}K_{\rm IC}$. This assumption implies that the ratio between the material strength and the fracture toughness for a homogeneous structure is the same as that for a heterogeneous one. In general, the higher the strength, the lower the fracture toughness for a given material. However, it is reasonable to expect the occurrence of this trend both in homogeneous and in graded materials, thus leading to $\sigma_{\rm u}\widetilde{K}_{\rm IC} \cong \widetilde{\sigma}_{\rm u}K_{\rm IC}$. In addition, since the classical application of the FE method to the computation of the stress-intensity factor in FGMs does not involve the specification of material strength and toughness, it is reasonable to assume that the generalized shape function in Eq. 14 is independent of these material parameters. In any case, this simplified hypothesis will be checked in the sequel by comparing the model predictions with FE results.

Brittle crack propagation can be predicted by means of the criterion $\widetilde{K}_{\rm I} = \widetilde{K}_{\rm IC}$. This general formulation can be then particularized to specific variations of the elastic modulus along the beam depth. The main equations for a linear grading as well as for a discrete grading have been derived and collected in the Appendix.

3 Fatigue in FGMs

In order to simulate fatigue crack growth in FGMs, the well-known Paris' law is adopted:

$$\frac{\mathrm{d}a}{\mathrm{d}N} = C\,(\Delta K_{\mathrm{I}})^{m}\,, \tag{15}$$

where ΔK_{I} denotes the variation in a cycle of the stress-intensity factor and N is the cycles number. Parameters C and m are experimental constants and the parameter m usually ranges between 1 and 4 for metals and between 10 and 100 for ceramics. Based on the computed values of the generalized stress-intensity factor $\widetilde{K}_{\mathrm{I}}$ at each crack length, and applying Eq. 15 with a step-by-step integration, the fatigue life of graded structures can be predicted.

In general, crack propagation under fatigue loading is influenced by the material gradient, due to the altered stress field throughout the loading cycle, and to the spatial variation in fatigue resistance. Due to the inherent complexity of the problem and the lack of extensive experimental data available in the Literature, constant Paris' law parameters are assumed in the simulations. This assumption, which may be reasonable for titanium alloys where the Paris' law parameters are weakly varying (Forth et al. 2004), permits to analyze the effect of the altered stress field due to the material gradient on the process of fatigue crack growth.

According to this hypothesis, we introduce two nondimensional quantities which characterize the mechanical response under fatigue crack propagation. The first parameter is defined as the ratio between the cycles number for a FGM structure corresponding to a given crack length, divided by the cycles number at failure for a structure having a homogeneous composition:

$$\frac{(N)^{\mathrm{FGM}}}{(N_{\max})^{\mathrm{HOM}}} = \frac{\int_{a_0}^{a} \frac{1}{C_{\mathrm{FGM}}\left(\Delta K_{\mathrm{I}}^{\mathrm{FGM}}\right)^{m_{\mathrm{FGM}}}}\,\mathrm{d}a}{\int_{a_0}^{a_{\mathrm{f}}} \frac{1}{C_{\mathrm{HOM}}\left(\Delta K_{\mathrm{I}}^{\mathrm{HOM}}\right)^{m_{\mathrm{HOM}}}}\,\mathrm{d}a}, \tag{16}$$

where a_0 and a_{f} denote, respectively, the initial and the final (at failure) crack lengths. In case of grading upon the elastic properties only, i.e., $C_{\mathrm{FGM}} = C_{\mathrm{HOM}}$ and $m_{\mathrm{FGM}} = m_{\mathrm{HOM}}$, Eq. 16 turns out to be independent of the Paris' law parameters C.

The second parameter is defined as the ratio between the velocity of crack propagation inside a FGM structure and the corresponding velocity inside a homogeneous one, under the same applied external loads:

$$\frac{v_{\mathrm{FGM}}}{v_{\mathrm{HOM}}} = \frac{\left.\frac{\mathrm{d}a}{\mathrm{d}N}\right|_{\mathrm{FGM}}}{\left.\frac{\mathrm{d}a}{\mathrm{d}N}\right|_{\mathrm{HOM}}} = \frac{C_{\mathrm{FGM}}\left(\Delta K_{\mathrm{I}}^{\mathrm{FGM}}\right)^{m_{\mathrm{FGM}}}}{C_{\mathrm{HOM}}\left(\Delta K_{\mathrm{I}}^{\mathrm{HOM}}\right)^{m_{\mathrm{HOM}}}}. \tag{17}$$

In case of grading upon the elastic properties only, i.e., $C_{\mathrm{FGM}} = C_{\mathrm{HOM}}$ and $m_{\mathrm{FGM}} = m_{\mathrm{HOM}}$, Eq. 17 simplifies as follows:

$$\frac{v_{\mathrm{FGM}}}{v_{\mathrm{HOM}}} = \left(\frac{\Delta K_{\mathrm{I}}^{\mathrm{FGM}}}{\Delta K_{\mathrm{I}}^{\mathrm{HOM}}}\right)^{m}. \tag{18}$$

Furthermore, if we consider $\Delta K_{\mathrm{I}} = K_{\mathrm{I}}^{\max} - K_{\mathrm{I}}^{\min} = \widetilde{K}_{\mathrm{I}}$ and the approximate expression for $\widetilde{K}_{\mathrm{I}}$ in Eqs. 4, then Eq. 18 can be further simplified as:

$$\frac{v_{\mathrm{FGM}}}{v_{\mathrm{HOM}}} \cong \left(\frac{\widetilde{g}}{g}\right)^{m}. \tag{19}$$

Due to these relationships, it is possible to compare the fatigue performance of a FGM structure with either continuous or discrete grading.

Finally, it has to be remarked that the proposed model can also be extended by considering a spatial variation in the Paris' law parameters. As regards the phenomenon of unstable crack growth, it is well-established that fracture toughness is dependent on the volumetric content of the constituent materials (Jin and Batra 1996). This dependence can be determined according to simplified mixture rules or using crack-bridging concepts (Jin and Batra 1996). On the other hand, concerning the phenomenon of fatigue crack growth, the problem is more complicated. Generally, two main classes of fatigue behaviors are reported in the Literature. In the first class, concerning FGMs with a composition ranging from ceramics to metals, the increase in the volumetric content of the ceramic particulates resulted in higher crack growth resistance with a retardation mechanism of fatigue crack growth (Xu et al. 2003). In the second class, concerning functionally graded titanium alloys, a different mechanism was observed. More specifically, it was noticed a transition from the Paris' law typical of the material composition present at the surface (with fine grains), to the Paris' curve of the material in the interior (with coarse grains).

These observations may suggest the possibility to have a dependence of the Paris' law parameters on the position (for the first class of materials) or on the stress-intensity factor range (for the second class of materials). Hence, the second effect related to the spatial variation in the fatigue resistance could be included in future improvements of the present model by considering variable Paris' law parameters in Eq. 15 based on specific experimental data.

4 Numerical assessment with the Finite Element method

In order to perform an assessment of the proposed approximate formulation, model results are compared with Finite Element predictions. Let us consider the three-point bending beam of Fig. 1b composed of two external homogeneous layers having elastic moduli E_3 and E_1, connected by an interlayer having a linear grading in the Young's modulus. In this case, the elastic modulus is assumed to be continuous along the whole beam height, i.e., $E_{23} = E_3$ and $E_{12} = E_1$.

Reference results for this case-study were numerically computed by Gu et al. (1999) according to a simplified Finite Element method based on the domain integral approach. In their model, two cases were considered, depending on the depth of the FGM layer. The thinner configuration is characterized by $h_1/h = h_3/h = 0.45$, $h_2/h = 0.10$ and $l/h = 5$, where h and l denote, respectively, the total depth and the span of the beam. For this problem, the parameter $K_I\sqrt{h/2}/P$ is depicted versus the nondimensional crack length $(a - h/2)/(h/2)$ in Fig. 2 for different values of the ratio between the elastic moduli E_3/E_1. It has to be remarked that the results in this diagram proposed by Gu et al. (1999) depend on the beam span. A direct comparison of Fig. 2a and b shows that the results obtained according to our simplified approach are in fair good agreement with the FE solution for ratios between the elastic moduli in the range from 0.05 to 5.

The other configuration with a thicker interlayer is characterized by $h_1/h = h_3/h = 0.25$, $h_2/h = 0.5$ and $l/h = 5$. In this case, the comparison proposed in Fig. 3 shows a rather good agreement between

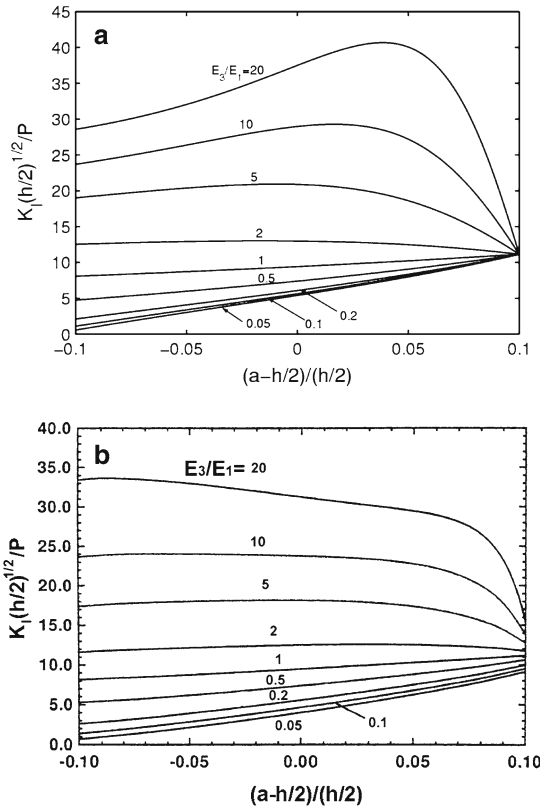

Fig. 2 Stress-intensity factor versus nondimensional crack length for the three-point bending beam of with $h_1/h = h_3/h = 0.45$, $h_2/h = 0.10$ and $l/h = 5$: (**a**) approximate results; (**b**) FE results reprinted from Gu et al. (1999)

our simplified approach and FE solutions over the whole range of variation of the elastic moduli.

A possible reason for major discrepancies between our proposed solution and reference FE results in the case of a thinner FGM layer can be due to the behavior of the structure when the first two external layers are completely cracked. Our model predicts that, when the crack propagates inside the last homogeneous layer, the stress-intensity factor equals that of a homogeneous beam, regardless of the elastic properties of the cracked layers. From FE simulations by Gu et al. (1999), it seems that the FGM interlayer with thickness $h_2/h = 0.10$ is not thick enough to exhibit this behavior.

In case of discrete grading, comparisons with FE results for a two-layer three-point bending beam (see the scheme depicted in Fig. 1c) can be found in Carpinteri et al. (2006). Also in this case, a close

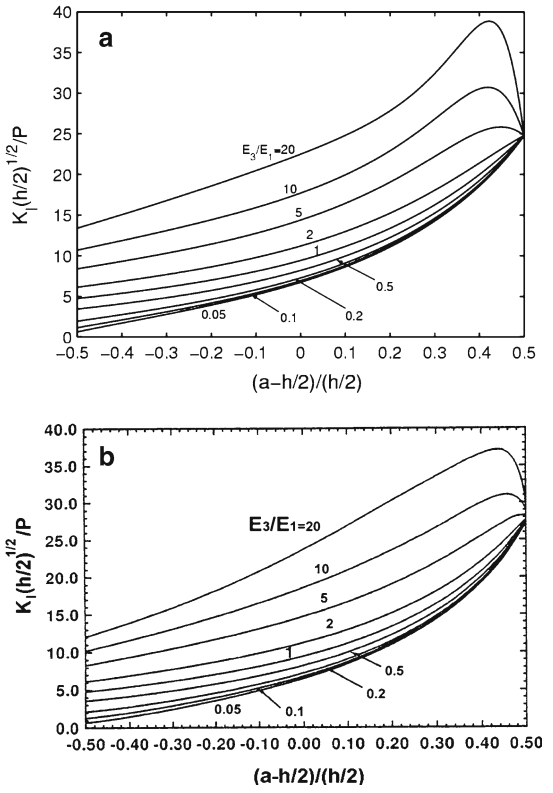

Fig. 3 Stress-intensity factor versus nondimensional crack length for the three-point bending beam of Fig. 2 with $h_1/h = h_3/h = 0.25$, $h_2/h = 0.50$ and $l/h = 5$: (**a**) approximate results; (**b**) FE results (reprinted from Gu et al. 1999)

agreement between the approximate generalized shape functions and the corresponding FE solution was noticed.

5 Comparison between continuous and discrete grading

In this section we aim at performing a comparison between the fracture behavior of three-point bending beams having either a continuous or a discrete grading. Two configurations are addressed: (1) a three-point bending beam made of three layers with an intermediate FGM interlayer; (2) a three-point bending beam made of two layers with an external FGM coating layer.

In the former case, a continuous linear grading implies that the elastic modulus of the FGM interlayer linearly connects the elastic moduli of the other layers. On the other hand, when a discrete grading is considered, the elastic modulus of the interlayer is set constant through the FGM depth and equal to the average value of the elastic moduli of the external layers (see Fig. 1b). Geometrical parameters of the beam are: $h_1/h = 0.60$, $h_2/h = h_3/h = 0.20$ and $l/h = 5$.

In the latter case, the thickness of the third layer is set equal to zero, i.e., $h_3 = 0$, and the other geometrical parameters are equal to $h_1/h = 0.60$, $h_2/h = 0.40$ and $l/h = 5$. In case of linear grading, the elastic modulus of the external layer linearly varies from $E_{23} = E_3$ to $E_{12} = E_1$. On the contrary, when a discrete grading is considered, the elastic modulus of this external layer is set constant and equal to $(E_1 + E_3)/2$ (see the scheme in Fig. 1c for the nomenclature used).

5.1 Three-point bending beam with a FGM interlayer

In case of brittle crack propagation, the fracture behavior is fully determined once the evolution of the generalized shape function versus the crack length is obtained. It has to be noticed that the diagram of the generalized shape function in terms of the nondimensional crack length is independent of the geometrical parameters of the beam. Then, this diagram should be preferred to that proposed by Gu et al. (1999) in which the solutions are dependent on the beam span. For this problem, results corresponding to linear and discrete grading are presented in Fig. 4a and b, respectively. In the former case, the linear variation of the elastic modulus in the FGM layer gives rise to a continuous generalized shape function over the whole beam depth. In general, due to grading, not only the elastic modulus, but also the critical stress-intensity factor can vary with position. In the special case where the toughness is constant over the FGM thickness, the crack growth is likely to be unstable for $E_3/E_1 \leq 1$ (see Fig. 4a). In such cases, if the condition for crack propagation is enforced at each step, i.e., $\widetilde{K}_{\mathrm{I}} = \widetilde{K}_{\mathrm{IC}}$ at the crack-tip, the external load has to be reduced during the crack propagation, since the shape function increases. On the other hand, according to the same reasoning, we observe from the same figure that, when

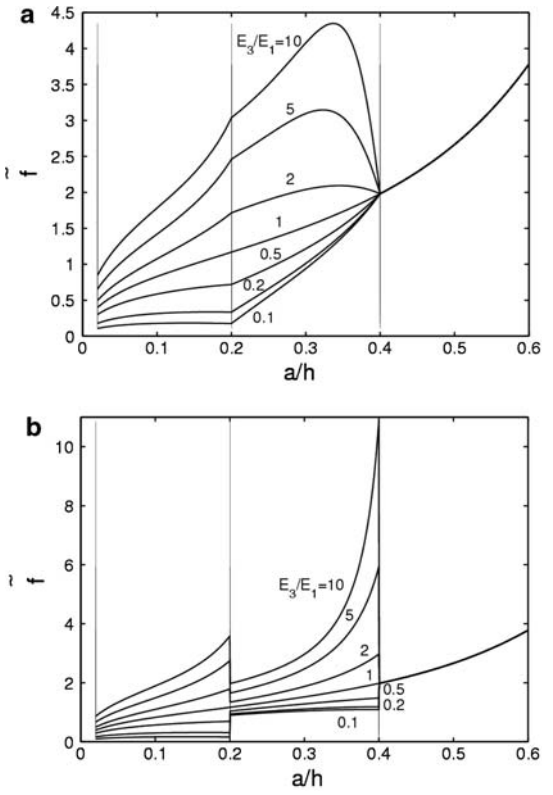

Fig. 4 Generalized shape function versus nondimensional crack length for the three-point bending beam of Fig. 2 with $h_1/h = 0.6$, $h_2/h = h_3/h = 0.20$ and $l/h = 5$: (**a**) continuous and (**b**) discrete gradings

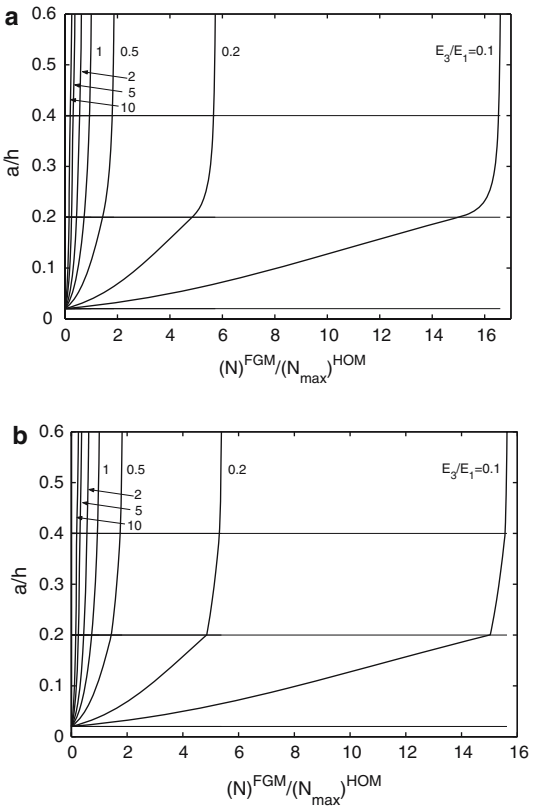

Fig. 5 Nondimensional crack length versus nondimensional cycles number for the three-point bending beam of Fig. 2 with $h_1/h = 0.6$, $h_2/h = h_3/h = 0.20$, $l/h = 5$ and $m_1 = m_{12} = m_{23} = m_3 = 1$: (**a**) continuous and (**b**) discrete gradings

$E_3/E_1 > 1$, crack propagation is unstable up to the crack length corresponding to the maximum of the shape function. When the shape function decreases after this maximum, a stable crack propagation may occur.

A completely different behavior is predicted in case of discrete grading, as shown in Fig. 4b. Generalized shape functions present discontinuities in correspondence of the bi-material interfaces. For a crack-tip approaching the bi-material interface in case of $E_3/E_1 > 1$, the generalized shape functions clearly increase with the crack length, because of the elastic mismatch. Unstable crack propagations are likely to occur in such cases. Furthermore, the maximum value reached by the shape function in case of $E_3/E_1 = 10$ with discrete grading is more than twice that for the corresponding problem with continuous grading.

Generalized shape functions for configurations having modular ratios E_3/E_1 less than unity slightly decrease when the crack-tip approaches the bi-material interfaces (see Fig. 4b). This implies that cracks are difficult to propagate across the bi-material interface when the substrate is stiffer than the coating. This result is in agreement with FE results obtained by Chi and Chung (2003).

As far as fatigue crack growth is concerned, a comparison in terms of the fatigue life for three-point bending beams with either continuous or discrete grading is proposed in Fig. 5. In order to investigate on the effect of the elastic grading only upon the fatigue life of the component, parameters C and m are assumed to be the same for each layer and we have set $m = 2$. The nondimensional crack length is depicted as a function of the nondimensional cycles number in Fig. 5.

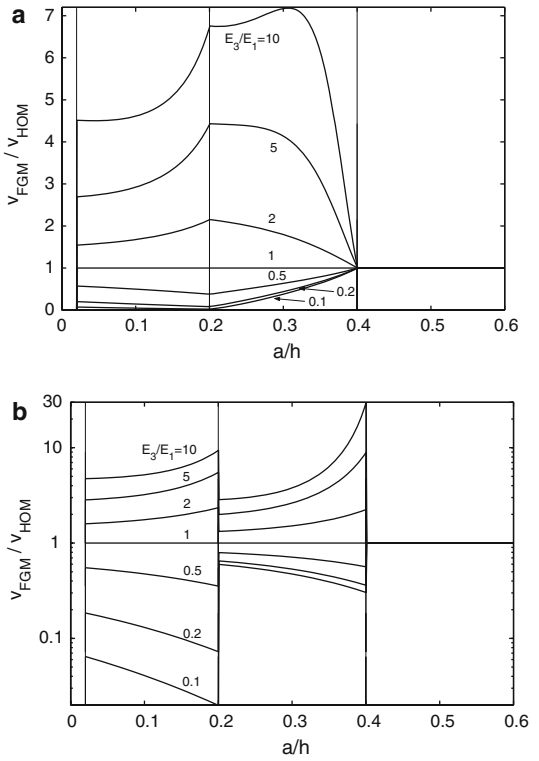

Fig. 6 Crack-tip velocity versus nondimensional crack length for the three-point bending beam of Fig. 2 with $h_1/h = 0.6$, $h_2/h = h_3/h = 0.20$, $l/h = 5$ and $m_1 = m_{12} = m_{23} = m_3 = 1$: (**a**) continuous and (**b**) discrete gradings

Independently of the type of grading being considered, we recognize that the softer the material 3 compared to the material 1, the longer the fatigue life. From a closer comparison between Fig. 5a and b it has to be noticed that, for any modular ratios, the fatigue life is approximately the same regardless of the type of grading adopted. Since the evolution of the crack length versus the cycles number is computed as the integral of the velocity of crack propagation estimated according to Eq. 15, the fact that the fatigue life is the same in the case of linear and discrete grading solutions implies that the average crack-tip velocity is approximately the same in both cases.

To fix ideas, let us consider the cases with E_3/E_1 higher than unity. For these problems, when the crack-tip is in the external layer, the velocity of crack propagation is approximately the same regardless of the type of grading (see Fig. 6). When the crack propagates inside the second layer, then the crack-tip velocity decreases down to that of a homogeneous beam if a linear variation in the elastic modulus is assumed. On the other hand, in case of discrete grading, a reduction of the crack-tip velocity occurs at the very beginning and then a sudden increase takes place when the crack-tip approaches the third layer. The velocity of crack propagation in the last homogeneous layer is the same in both cases. As a result, the average velocity of crack propagation is almost the same in both types of grading and the discrete grading approach seems to be as effective as the continuous counterpart when fatigue crack growth is the dominant fracture mechanism.

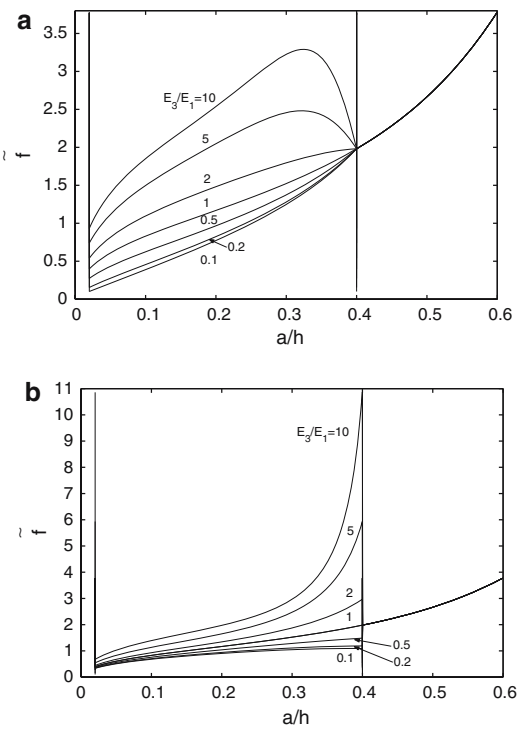

Fig. 7 Generalized shape function versus nondimensional crack length for the three-point bending beam of Fig. 3 with $h_1/h = 0.6$, $h_2/h = 0.4$, $h_3/h = 0.0$ and $l/h = 5$: (**a**) continuous and (**b**) discrete gradings

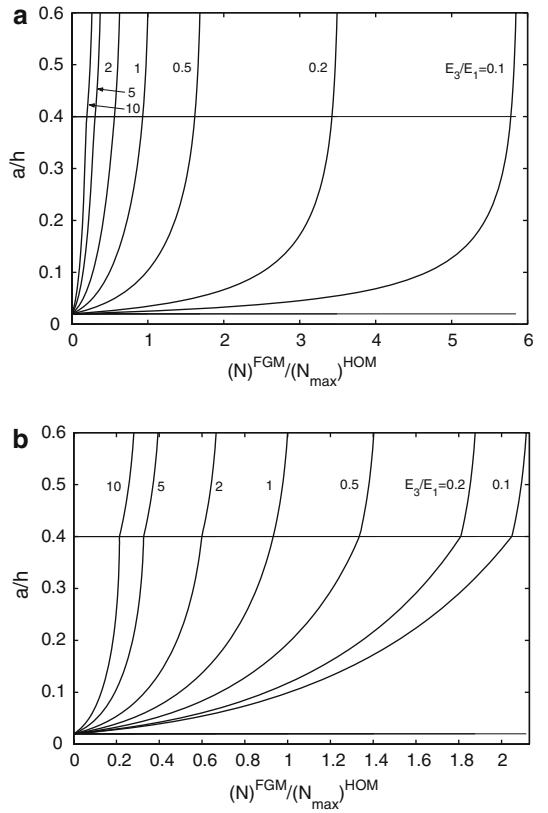

Fig. 8 Nondimensional crack length versus nondimensional cycles number for the three-point bending beam of Fig. 3 with $h_1/h = 0.6$, $h_2/h = 0.4$, $h_3/h = 0.0$, $l/h = 5$ and $m_1 = m_{12} = m_{23} = m_3 = 1$: (**a**) continuous and (**b**) discrete gradings

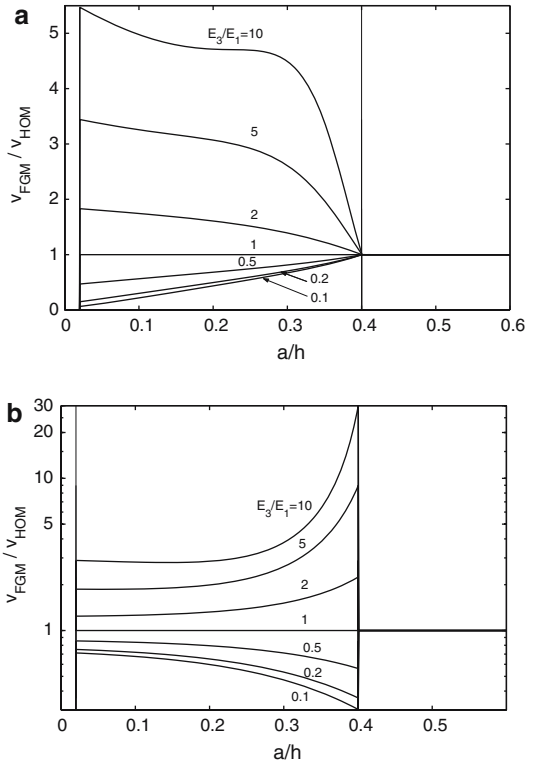

Fig. 9 Crack-tip velocity versus nondimensional crack length for the three-point bending beam of Fig. 3 with $h_1/h = 0.6$, $h_2/h = 0.4$, $h_3/h = 0.0$, $l/h = 5$ and $m_1 = m_{12} = m_{23} = m_3 = 1$: (**a**) continuous and (**b**) discrete gradings

5.2 Three-point bending beam with an external FGM layer

In case of brittle crack propagation, the generalized shape functions corresponding to both linear and discrete grading are shown in Fig. 7a and b, respectively. The previous considerations about the shape of these curves and the stability of crack propagation hold also for this case.

On the other hand, a different behavior has to be noticed in case of fatigue crack growth. In order to investigate on the effect of the elastic grading only upon the fatigue life of the component, we have assumed the same values for C and m for the two layers and we have set $m = 2$, as in the previous examples. The nondimensional crack length is depicted as a function of the nondimensional cycles number in Fig. 8. Independently of the type of grading being considered, the softer the material 3 compared to the material 1, the longer the fatigue life. Furthermore, we observe that the predicted fatigue life is comparable for both types of grading when $E_3/E_1 \geq 1$. On the other hand, when $E_3/E_1 < 1$, the fatigue life in case of a linear grading is longer than that corresponding to the case of discrete grading. For instance, when $E_3/E_1 = 0.1$, the relative gain in the fatigue life is approximately equal to three times. This trend is expected to increase if higher values of m are considered.

For the sake of completeness, the corresponding crack-tip velocities are depicted in Fig. 9 as functions of the nondimensional crack length.

6 Conclusions

The problem of brittle crack propagation and fatigue crack growth in FGMs has been addressed. The simplified analytical approach herein presented can be used to investigate on Mode I crack propagation. The problems of a beam under three-point bending and of a finite plate in tension with edge cracks are noticeable examples that can be tackled with this approach by using the well-known shape functions reported in the fracture mechanics handbooks.

The main formulae have been specified to the case of three-point bending beams with either two or three layers. The simplified assumptions have been checked by comparing the model results with FE solutions and a good agreement has been noticed.

Focusing our attention on the comparison between discrete and continuous grading solutions, generalized shape functions have been derived. These solutions characterize the problem of brittle crack propagation. It has been observed that linear grading is particularly effective in the reduction of the stress-intensity factor for cracks close to the bi-material interfaces. Also, stable crack propagations may occur when a linear grading is considered due to the observed decreasing stress-intensity factor in a given range of crack depths.

As regards the phenomenon of fatigue crack propagation, the crack-tip velocity and the cycles number have been predicted in terms of the crack length by assuming constant parameters entering the Paris' law. This assumption, which may be reasonable for functionally graded titanium alloys where the Paris' law parameters are weakly varying from 3.40 to 4.33 (Forth et al. 2003), has permitted to focus the attention on the effect of the altered stress field due to the material gradient on the process of fatigue crack growth. Linear and discrete grading are almost equivalent in case of three-point bending beams with a FGM interlayer. In such situations, the fatigue life is mainly ruled by the external layer and the average crack-tip velocities are approximately the same regardless of the type of grading solution being considered. A completely different behavior occurs when the problem of a two-layers three-point bending beam with an external FGM layer is addressed. In these cases, the life is longer when a continuous grading solution is adopted. Moreover, it has to be noticed that a grading in the fatigue parameters can also be taken into account in a future improvement of the model by considering a spatial variation in the fatigue resistance according to specific experimental data.

As compared to the well-established weight function method (see e.g., Fett and Munz (1997) and thereafter) which permits to accurately determine the stress-intensity factor in FGMs and in multi-layered elements, the herein proposed approach presents several advantages. First of all, it has to be remarked that the weight function method requires the determination of the weight functions that are dependent not only on the geometry, but also of the elastic constants of the joint (see Fett et al. 1997), thus leading to relatively complicated expressions. Conversely, the approximate solution proposed in the present paper permits to determine the generalized shape function for a heterogeneous structural element just starting from the simple expressions of the shape functions for the limit homogeneous cases available in the fracture mechanics handbooks. Hence, this simplified approach can be particularly effective from the engineering point of view, since the results can be used to draw a first guideline for the design of structural elements with functionally graded materials.

7 Appendix

Functionally graded materials are usually used either as an external coating layer, or as a strip sandwiched between two homogeneous layers of finite thickness. Hence, the expressions of the weighted moment of inertia, $\widetilde{I}_x^*$, given by Eq. 10, and of the co-ordinate of the crack-tip with respect to origin of the reference system defined by Eq. 11, $\widetilde{y}$, are herein particularized to handle with these important applications. Closed form equations are provided both for the case of a continuous (linear) grading, and for a discrete (multi-layered) solution.

7.1 Continuous grading

Let a three-point bending beam be composed of three layers (see the scheme in Fig. 1b). The extreme layers are homogeneous and are referred to as layer 1 and 3, respectively. Their elastic moduli are denoted by E_1 and E_3. These layers are joined by a FGM strip with a linear grading in the elastic modulus. For the sake of generality, the values of the elastic moduli of the FGM layer at the interfaces, i.e., E_{12} and E_{23}, can be different from those of the homogeneous layers.

According to Eqs. 10 and 11, it is possible to compute the position of the crack-tip with respect to the origin of the reference system and the weighted moment of inertia. In case of an uncracked structure, i.e., for $a = 0$, we have $\widetilde{E} = E_3$ and:

$$\widetilde{y} = \frac{h_1\left(\frac{h_1}{2}+h_2+h_3\right)+\frac{E_{23}}{E_1}h_2\left(h_3+\frac{h_2}{2}\right)+\frac{h_2}{2}\left(\frac{E_{12}}{E_1}-\frac{E_{23}}{E_1}\right)\left(h_3+\frac{2}{3}h_2\right)+\frac{E_3}{E_1}\frac{h_3^2}{2}}{h_1+h_2\frac{E_{23}}{E_1}+\frac{h_2}{2}\left(\frac{E_{12}}{E_1}-\frac{E_{23}}{E_1}\right)+\frac{E_3}{E_1}h_3}$$

$$\widetilde{I}_x^* = \frac{E_1}{\widetilde{E}}b\left\{\frac{h_1^3}{12}+h_1\left(\frac{h_1}{2}+h_2+h_3-\widetilde{y}\right)^2 + \frac{E_{23}}{E_1}\left[\frac{h_2^3}{12}+h_2\left(\frac{h_2}{2}+h_3-\widetilde{y}\right)^2\right] + \left(\frac{E_{12}}{E_1}-\frac{E_{23}}{E_1}\right)\left[\frac{h_2^3}{36}+\frac{h_2}{2}\left(\frac{2}{3}h_2+h_3-\widetilde{y}\right)^2\right] + \frac{E_3}{E_1}\left[\frac{h_3^3}{12}+h_3\left(\frac{h_3}{2}-\widetilde{y}\right)^2\right]\right\} \quad (20)$$

The formulation is completed by noting that the corresponding values for a cross-section reduction due to the presence of a crack of length a, i.e., $\widetilde{y} = \widetilde{y}(a)$ and $\widetilde{I}_x^* = \widetilde{I}_x^*(a)$, can be obtained from the previous two relationships with the following substitutions, depending on the crack depth:

$$\begin{array}{ll} a < h_3 & \widetilde{E} = E_3, h_3 \Longrightarrow h_3 - a \\ h_3 \le a < h_2 + h_3 & \widetilde{E} = (E_{12} - E_{23})\frac{a-h_3}{h_2} + E_{23}, \\ & E_{23} \Longrightarrow \widetilde{E}, h_2 \Longrightarrow h_2 + h_3 - a, \\ & h_3 \Longrightarrow 0 \\ a \ge h_2 + h_3 & \widetilde{E}{=}E_1, h_1 \Longrightarrow h_1 + h_2 + h_3 - a, \\ & h_2 \Longrightarrow 0, h_3 \Longrightarrow 0 \end{array} \quad (21)$$

The problem of a two-layered beam with an external FGM layer can be derived as a limit case by setting $h_3 = 0$ in the above equations:

$$\widetilde{y} = \frac{h_1 h_2 + \frac{h_1^2}{2} + \frac{h_2^2 E_{23}}{2E_1} + \left(\frac{E_{12}}{E_1} - \frac{E_{23}}{E_1}\right)\frac{h_2^2}{3}}{h_1 + \frac{h_2 E_{23}}{E_1} + \left(\frac{E_{12}}{E_1} - \frac{E_{23}}{E_1}\right)\frac{h_2}{2}}, \quad (22)$$

$$\hat{I}_x^* = \frac{E_1}{\widetilde{E}}b\left\{\frac{h_1^3}{12}+h_1\left(h_2+\frac{h_1}{2}-\widetilde{y}\right)^2 + \frac{E_{23}}{E_1}\left(\frac{h_2^3}{3}+\widetilde{y}^2 h_2 - \widetilde{y}h_2^2\right) + \left(\frac{E_{12}}{E_1}-\frac{E_{23}}{E_1}\right)\left(\frac{h_2^3}{4}+\widetilde{y}^2\frac{h_2}{2}-2\widetilde{y}\frac{h_2^2}{3}\right)\right\} \quad (23)$$

Also in this case, the corresponding values for a cross-section reduction due to the presence of a crack of length a, $\widetilde{y} = \widetilde{y}(a)$ and $\widetilde{I}_x^* = \widetilde{I}_x^*(a)$, can be obtained by substitution:

$$\begin{array}{l} a < h_2 \; E_2 \Longrightarrow \hat{E}, h_2 \Longrightarrow h_2 - a \\ a \ge h_2 \; E_1 \Longrightarrow \hat{E}, h_2 \Longrightarrow 0, \; h_1 \Longrightarrow h_1 + h_2 - a \end{array} \quad (24)$$

7.2 Discrete grading

In certain applications, the use of a multi-layered beam instead of a structure with continuous grading can be motivated by technological and economical reasons. Therefore, in such cases, a comparison of the corresponding fracture behaviors can be particularly useful for design and optimization procedures. In this case, the weighted static moment of the rectangular ligament cross-section with respect to a given axis can be written as:

$$S_x^* = \frac{b}{\widetilde{E}}\sum_{i=1}^{N} E_i h_i y_{Gi}, \quad (25)$$

where h_i are the depths of the N layers composing the ligament cross-section, b denotes their common width and y_{Gi} is the co-ordinate of the geometrical centroid for the i-th layer. The Young's

modulus of the i-th layer is E_i, whereas $\widetilde{E}$ is the Young's modulus of the material at the crack-tip. From geometrical considerations we have:

$$y_{Gi} = \widetilde{y} - \sum_{j=1}^{i} h_j + \frac{h_i}{2} \tag{26}$$

where $\widetilde{y}$ represents the distance between the origin of the chosen reference system ($y = 0$) and the crack-tip. Introducing Eq. 20 into Eq. 19 and imposing a vanishing weighted static moment, the distance $\widetilde{y}$ between the weighted centroid of the ligament cross-section and the crack-tip is derived:

$$\widetilde{y} = \frac{\sum_{i=1}^{N} \left\{ E_i h_i \left(\sum_{j=1}^{i} h_j - \frac{h_i}{2} \right) \right\}}{\sum_{i=1}^{N} E_i h_i} \tag{27}$$

Eventually, the weighted moment of inertia with respect to the elastic centroid axis can be obtained:

$$I_x^* = \frac{b}{E_r} \sum_{i=1}^{N} E_i \left\{ \frac{h_i^3}{12} + b_i \left(\frac{\sum_{i=1}^{N} \left\{ E_i h_i \left(\sum_{j=1}^{i} h_j - \frac{h_i}{2} \right) \right\}}{\sum_{i=1}^{N} E_i h_i} - \sum_{j=1}^{i} h_j + \frac{h_i}{2} \right)^2 \right\} \tag{28}$$

As a result, the shape function and the stress-intensity factor at the crack-tip in a multi-layered structure can be evaluated according to Eq. 14.

Acknowledgements Support by the Italian Ministry of University and Research (MIUR) is gratefully acknowledged.

References

Carpinteri A (1982) Notch sensitivity in fracture testing of aggregative materials. Eng Fract Mech 16:467–481

Carpinteri A (1987) Stress-singularity and generalized fracture toughness at the vertex of re-entrant corners. Eng Fract Mech 26:143–155

Carpinteri A (1997) Structural mechanics: a unified approach. Chapman & Hall, London

Carpinteri A, Paggi M (2005) On the asymptotic stress field in angularly nonhomogeneous materials. Int J Fract 135:267–283

Carpinteri A, Pugno N (2005) Fracture instability and limit strength condition in structures with re-entrant corners. Eng Fract Mech 72:1254–1267

Carpinteri A, Pugno N (2006) Cracks and re-entrant corners in functionally graded materials. Eng Fract Mech 73:1279–1291

Carpinteri A, Paggi M, Pugno N (2006) Numerical evaluation of generalized stress-intensity factors in multi-layered composites. Int J Solids Struct 43:627–641

Chawla KK (1987) Composite materials: science and engineering. Springer-Verlag, NewYork, Berlin, Heidelberg, London, Paris, Tokyo

Chi S-H, Chung Y-L (2003) Cracking in coating-substrate composites with multi-layered and FGM coatings. Eng Fract Mech 70:1227–1243

Delale F, Erdogan F (1983) The crack problem for a non-homogeneous plane. ASME J Appl Mech 50:609–614.

Eischen JW (1987) Fracture of nonhomogeneous materials. Int J Fract 34:3–22

Erdogan F (1995) Fracture mechanics of functionally gradient materials. Compos Eng 5:753–770

Erdogan F, Wu BH (1997) The surface crack problem for a plate with functionally graded properties. ASME J Appl Mech 64:449–456

Fett T, Munz D (1997) Stress intensity factors and weight functions. Computational Mechanics Publications, Southampton

Fett T, Tilscher, Munz D (1997) Weight functions for cracks near the interface of a bimaterial joint, and application to thermal stresses. Eng Fract Mech 56:87–100.

Forth SC, Favrow LH, Keat WD, Newman JA (2003) Three-dimensional mixed-mode fatigue crack growth in a functionally graded titanium alloy. Eng Fract Mech 70:2175–2185

Gu P, Dao M, Asaro RJ (1999) A simplified method for calculating the crack-tip field of functionally graded materials using the domain integral. ASME J Appl Mech 66:101–108

Jin Z-H, Batra RC (1996) Some basic fracture mechanics concepts in functionally graded materials. J Mech Phys Solids 44:1221–1235

Kim J-H, Paulino GH (2002) Mixed-mode fracture of orthotropic functionally graded materials using finite elements and the modified crack closure method. Eng Fract Mech 69:1557–1586

Kim J-H, Paulino GH (2003) T-stress, mixed-mode stress intensity factors, and crack initiation angles in functionally graded materials: a unified approach using the interaction integral method. Comput Methods Appl Mech Eng 192:1463–1494

Murakami Y (ed) (1987) Stress intensity factors handbook. Pergamon, Oxford

Paulino GH (ed) (2002) Fracture of functionally graded materials. Eng Fract Mech 69:14–16

Xu FM, Zhu SJ, Zhao J, Qi M, Wang FG, Li SX, Wang ZG (2003) Fatigue crack growth in SiC particulates reinforced Al matrix graded composite. Mater Sci Eng A 360:191–196.